

Thermal-conductivity anisotropy of single-crystal $\text{Bi}_2\text{Sr}_2\text{CaCu}_2\text{O}_8$

M. F. Crommie and A. Zettl

*Department of Physics, University of California at Berkeley, and Materials and Chemical Sciences
Division of the Lawrence Berkeley Laboratory, Berkeley, California 94720*

(Received 20 June 1990)

We have measured the out-of-plane (c -axis) thermal conductivity κ_c of single-crystal $\text{Bi}_2\text{Sr}_2\text{CaCu}_2\text{O}_8$ from room temperature to 40 K. In contrast to the previously measured in-plane thermal conductivity κ_{ab} , κ_c appears to be phonon dominated and shows no dramatic anomaly at the superconducting transition temperature T_c . In the normal state above T_c , the electrical conductivity anisotropy σ_{ab}/σ_c is of order 10^4 and is strongly temperature dependent, while $\kappa_{ab}/\kappa_c \approx 6$, independent of temperature. Our results suggest an important role played by defect scattering in the c -axis transport mechanism of $\text{Bi}_2\text{Sr}_2\text{CaCu}_2\text{O}_8$.

Anisotropic transport remains a unifying feature in the highest- T_c oxide superconductors. Normal-state properties, such as the large anisotropy and unusual temperature dependence of the electrical conductivity,^{1,2} remain unexplained but have implications for the electrical ground state of this class of materials.³ In the superconducting state, anisotropic thermal conductivity measurements can be used to study anisotropic electron-phonon coupling and carrier scattering mechanisms.⁴⁻⁸

We here report on measurements of the out-of-plane (c -axis) thermal conductivity of single-crystal specimens of the $T_c = 85$ K oxide superconductor $\text{Bi}_2\text{Sr}_2\text{CaCu}_2\text{O}_8$ in the temperature range from room temperature to 40 K. Measurements of the anisotropic electrical resistivity tensor were also performed on crystals from the same preparation batch in order to quantitatively separate the thermal conductivity into phonon and electron terms. When κ_c is compared to previous measurements⁶ of the in-plane (ab -plane) thermal conductivity κ_{ab} on similar $\text{Bi}_2\text{Sr}_2\text{CaCu}_2\text{O}_8$ crystals, we find above T_c a thermal conductivity anisotropy $\kappa_{ab}/\kappa_c \approx 6$. This contrasts sharply with the much stronger electrical conductivity anisotropy $\sigma_{ab}/\sigma_c \approx 10^4$. κ_c appears to be phonon dominated, and shows no dramatic anomaly at T_c . This is in contrast to κ_{ab} in $\text{Bi}_2\text{Sr}_2\text{CaCu}_2\text{O}_8$ which has a substantial electron contribution and shows a large "bump" anomaly just below T_c . Analysis of our thermal and electrical conductivity data suggests an important role played by defect scattering in the c -axis conduction mechanism.

The $\text{Bi}_2\text{Sr}_2\text{CaCu}_2\text{O}_8$ single crystals were prepared as described elsewhere,⁹ and characterized by x -ray-scattering, magnetic susceptibility, and electrical resistivity studies.¹⁰ Resistive and magnetic T_c 's were typically 85 K with transition widths of a few K. The crystals were cleaved into thin ab -plane sheets roughly 1 mm on a side and 5–10 μm thick in the c direction.

We initially attempted to measure κ_c using an experimental configuration⁶ nearly identical to that used successfully for κ_{ab} measurements on similar crystals. However, it was found that the results were not reproducible upon temperature cycling, and "jumps" in the thermal

conductivity were observed. This was attributed to microcracking along the Bi-O planes of the crystal, induced by temperature-dependent c -axis stresses on the sample from the attached thermal source and sink leads. To counteract this problem, a specially constructed "thermal clamp cell" was used, shown schematically in the inset of Fig. 1. The cell consists of a calibrated Constantan thermal source rod attached to the ab -plane face of a small $\text{Bi}_2\text{Sr}_2\text{CaCu}_2\text{O}_8$ crystal. A spring-loaded copper thermal sink rod was attached to the opposite sample face. The relatively weak pressure supplied by the sink rod spring was effective in preventing "delamination" of the crystal along the c -axis. Silver paint was used to ensure good thermal contact between the sample and the source and sink rods. The actual measurement was performed using a steady-state comparative technique,⁶ where the temperature gradient developed across the sample was measured directly with a miniature differential thermocouple, attached to the sample faces with a very small amount of electrically insulating stycast epoxy. The differential thermocouple junctions were glued as close to the "clamped" region of the crystal as possible without touching the thermal source and sink rods, yielding a four-point thermal conductivity measurement. Error due to radiation and heat leads through the wires was estimated to be only a few percent. This method was found to be extremely reliable, and the sample could be thermally cycled repeatedly with good reproducibility.

Figure 1(a) shows the temperature dependence of the c -axis thermal conductivity of $\text{Bi}_2\text{Sr}_2\text{CaCu}_2\text{O}_8$. At room temperature $\kappa_c = 0.87$ W/mK, which is approximately a factor of 6 smaller than κ_a measured at room temperature on similar $\text{Bi}_2\text{Sr}_2\text{CaCu}_2\text{O}_8$ crystals.⁶ The temperature dependence shows that κ_c is fairly linear with a small positive slope (8.1×10^{-4} W/mK²) from room temperature down to ~ 135 K, at which point there is a barely discernible break in slope. κ_c takes a much sharper downturn just below ~ 70 K. It is important to note that this sharp downturn is *not* directly associated with the superconducting transition temperature of this crystal

(shown as a dashed vertical line; see discussion below), nor does it correspond to the peak in the "bump" structure observed in κ_{ab} of similar crystals (this occurs at $T \approx 62$ K). Indeed, Fig. 1(a) shows that as the temperature is lowered the out-of-plane thermal conductivity monotonically decreases, and shows no feature that correlates to the dramatic upturn and consequent bump structure of κ_{ab} of $\text{Bi}_2\text{Sr}_2\text{CaCu}_2\text{O}_8$ single crystals (and κ measured in polycrystalline specimens¹¹). The lack of any dramatic structure in κ_c is consistent with recent thermal diffusivity experiments¹² in $\text{Bi}_2\text{Sr}_2\text{CaCu}_2\text{O}_8$, and is similar to the out-of-plane thermal conductivity behavior observed in $\text{YBa}_2\text{Cu}_3\text{O}_7$ (Ref. 4) and $\text{La}_{1.96}\text{Sr}_{0.04}\text{CuO}_4$ (Ref. 5).

To identify unambiguously the T_c for the crystal used for the κ_c measurements in Fig. 1(a), an ac susceptibility measurement was performed on the same crystal. Figure 1(b) shows χ_{ac} versus T . The transition midpoint is obtained at $T_c = 85$ K, consistent with resistivity measurements on other samples from the same preparation batch. This confirms that κ_c in $\text{Bi}_2\text{Sr}_2\text{CaCu}_2\text{O}_8$ shows no outstanding structure at T_c .

In analyzing the c axis thermal transport and anisotropy

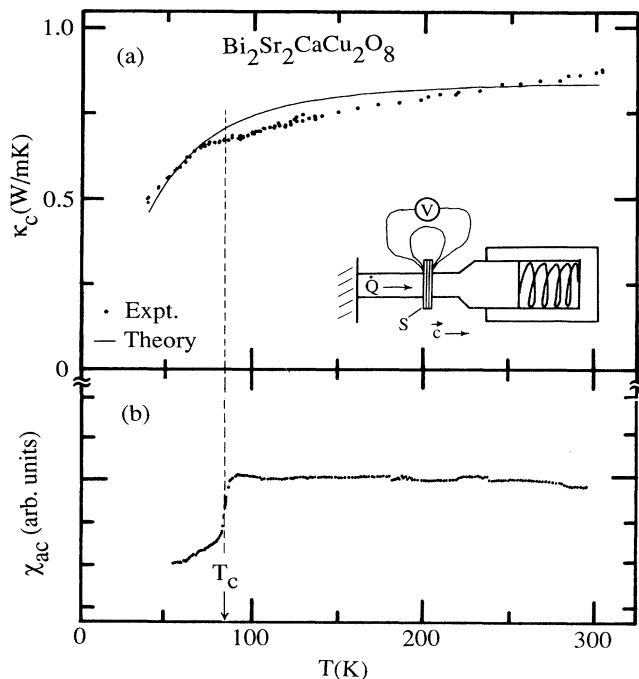


FIG. 1. (a) Measured c -axis thermal conductivity κ_c versus temperature for $\text{Bi}_2\text{Sr}_2\text{CaCu}_2\text{O}_8$. The superconducting transition temperature $T_c = 85$ K is indicated by a dashed vertical line. No obvious anomaly in κ_c is observed near T_c . The solid line is a fit to the theory of Tewordt and Wölkhausen, Eq. (2), with stacking faults as the dominant phonon scatters (fitting parameters given in the text). The inset shows the sample (S) mounting configuration for the κ_c measurements. (b) ac magnetic susceptibility shown in (a). The superconducting transition temperature is indicated by a vertical arrow.

in $\text{Bi}_2\text{Sr}_2\text{CaCu}_2\text{O}_8$ crystals, it is desirable to have accurate measurements of the electrical transport on similar crystals (with similar defect structure, etc.). Figure 2 shows both the in-plane and out-of-plane electrical resistivity of $\text{Bi}_2\text{Sr}_2\text{CaCu}_2\text{O}_8$ as functions of temperature. These data were obtained using a modification of the standard Montgomery method.¹³ The contact geometry, shown in the inset of Fig. 2, consists of four parallel silver paint strips, with each strip placed along an edge of the two opposite ab -plane faces of the crystal, and all four strips perpendicular to the c axis. The utility of the strips (as opposed to point contacts) is that they effectively "short out" the third dimension of the crystal, thus allowing application of the straightforward thin-plate-geometry Montgomery analysis. Although the c -axis direction of the crystal was well defined, no attempt was made here to distinguish between the a and b directions. The ab -plane resistivity measured and displayed in Fig. 2 thus corresponds to an arbitrary direction in the ab plane. Our main interest is in an accurate determination of ρ_c , and the temperature dependence of the extreme anisotropy in ρ_{ab}/ρ_c (the in-plane electrical anisotropy is known to be very small, less than 1.5 at room temperature²).

Figure 2 shows that the in-plane resistivity ρ_{ab} is linear down to 100 K with a small residual resistivity $< 20 \mu\Omega \text{ cm}$, in agreement with previous measurements by several groups. Below 100 K the resistivity begins to deviate from linear behavior, due possibly to fluctuation effects. The midpoint of the transition is at $T_c \sim 85$ K while $\rho = 0$ is reached at $T_{cf} \sim 80$ K. The out-of-plane resistivity ρ_c is considerably different. At room temperature ρ_c is more than four orders of magnitude larger than ρ_{ab} . ρ_c also does not display a linear temperature dependence, but rather shows a semiconductorlike upturn at lower temperatures, similar to that seen^{1,14} in the c -axis resistivity of some specimens of $\text{YBa}_2\text{Cu}_3\text{O}_{7-y}$. ρ_c abruptly turns over at $T \sim 82$ K and drops to zero at the

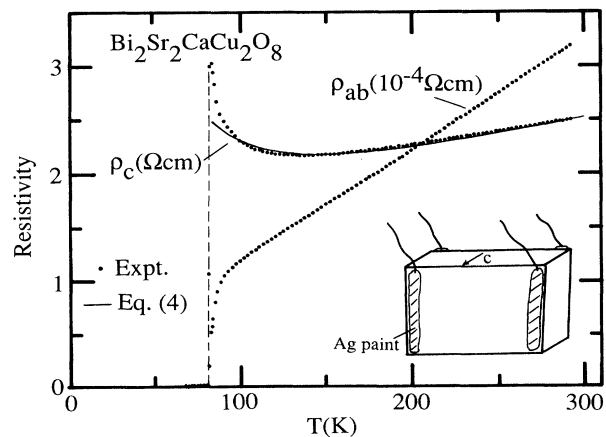


FIG. 2. ab -plane and c -axis electrical resistivity of $\text{Bi}_2\text{Sr}_2\text{CaCu}_2\text{O}_8$; note the different scales used. The dashed line is a guide to the eye for the c axis data near T_c . The solid line is a fit of ρ_c to Eq. (4), with fitting parameters given in the text. The inset shows the sample lead mounting configuration.

same temperature as does ρ_{ab} . We note that our observed anisotropy in ρ_{ab}/ρ_c is comparable to that determined previously.^{2,15} The functional form of ρ_c in Fig. 2, however, is different from that shown in Refs. 2 and 15 which report temperature-dependent c -axis resistivities that are either of a more “metallic”² or a more “semiconducting”¹⁵ nature.

Figure 3 shows the temperature dependence of the ratios of the in-plane to out-of-plane thermal and electrical conductivities of $\text{Bi}_2\text{Sr}_2\text{CaCu}_2\text{O}_8$, where κ_{ab} has been obtained from Ref. 6. Figure 3(a) shows the ratio of κ_{ab} to κ_c . The anisotropy ratio remains essentially constant at $\kappa_{ab}/\kappa_c \sim 6$ from room temperature down to $T_c \sim 85$ K. Below T_c the ratio rises steeply in response to a sharp increase in κ_{ab} as superconductivity sets in. For $T \leq 60$ K the ratio begins to level out at $\kappa_{ab}/\kappa_c \sim 8$, as κ_{ab} and κ_c both have a positive slope in this temperature range. Single-crystal $\text{YBa}_2\text{Cu}_3\text{O}_{7-y}$ and $\text{La}_{1.96}\text{Sr}_{0.04}\text{CuO}_4$ both show similar behavior, with room-temperature thermal conductivity anisotropies of 4.5 and 3, respectively.^{4,5} Figure 3(b) shows the ratio of the in-plane to out-of-plane electrical conductivity, σ_{ab}/σ_c . The anisotropy rises relatively slowly from $\sigma_{ab}/\sigma_c \sim 0.8 \times 10^4$ at room temperature to $\sigma_{ab}/\sigma_c \sim 1.9 \times 10^4$ at $T \sim 100$ K. Over the next 15 K, however, the anisotropy increases at a much higher rate to $\sigma_{ab}/\sigma_c \sim 5.7 \times 10^4$ at $T \sim 82$ K. It is interesting

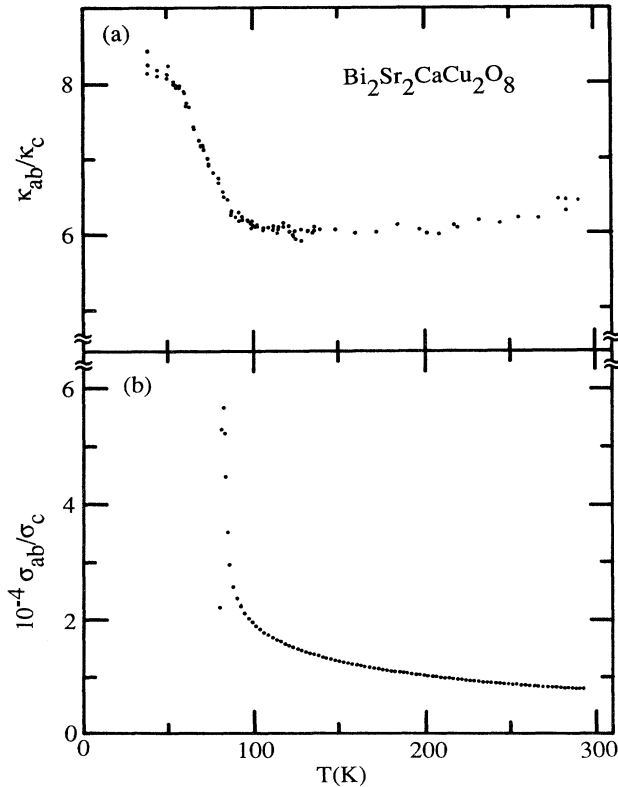


FIG. 3. (a) Ratio of measured ab -plane to c -axis thermal conductivity in $\text{Bi}_2\text{Sr}_2\text{CaCu}_2\text{O}_8$. The thermal conductivity anisotropy is nearly temperature independent in the normal state above $T_c = 85$ K. (b) Electrical conductivity anisotropy in $\text{Bi}_2\text{Sr}_2\text{CaCu}_2\text{O}_8$.

to note that $\text{YBa}_2\text{Cu}_3\text{O}_{7-y}$, while having a comparable thermal conductivity anisotropy to $\text{Bi}_2\text{Sr}_2\text{CaCu}_2\text{O}_8$, has an electrical anisotropy two orders of magnitude smaller.¹

In analyzing thermal conductivity data, it is desirable to separate κ_c into different carrier contributions and identify important scattering mechanisms. We here limit ourselves to electrons and phonons as the heat carriers in $\text{Bi}_2\text{Sr}_2\text{CaCu}_2\text{O}_8$. From the Wiedemann-Franz law the electron contribution $\kappa_{c(\text{electron})}$ to the total c -axis thermal conductivity κ_c is given by

$$\kappa_{c(\text{electron})} = \sigma_c \pi^2 k_B^2 T / 3e^2. \quad (1)$$

From Eq. (1) and the data of Figs. 1(a) and 2, we find $\kappa_{c(\text{electron})} \sim 3.0 \times 10^{-4}$ W/mK at room temperature and $\kappa_{c(\text{electron})} \sim 2.5 \times 10^{-4}$ W/mK just above $T_c = 85$ K. Hence, throughout the normal-state temperature range, κ_c is dominated by heat carried by phonons. This is in contrast to κ_{ab} in $\text{Bi}_2\text{Sr}_2\text{CaCu}_2\text{O}_8$, where approximately one-third of the heat is carried by electrons.⁶ A similar phonon-dominated out-of-plane thermal conductivity is found^{4,5} in $\text{YBa}_2\text{Cu}_3\text{O}_7$ and $\text{La}_{1.96}\text{Sr}_{0.04}\text{CuO}_4$. In $\text{La}_{1.96}\text{Sr}_{0.04}\text{CuO}_4$ the in-plane thermal conductivity also appears to be phonon dominated; in $\text{YBa}_2\text{Cu}_3\text{O}_7$ electrons contribute to over half the total in-plane thermal conductivity.

The lack of any anomaly in κ_c near T_c in $\text{Bi}_2\text{Sr}_2\text{CaCu}_2\text{O}_8$ has important consequences. The “bump” feature observed in κ_{ab} has been interpreted as providing evidence of phonons being strongly scattered by electrons (and in principle the detailed shape of the anomaly can be used to extract λ_{ab} , the in-plane electron-phonon coupling constant).⁷ The absence of such an anomaly in the measured κ_c suggests that either the phonons carrying heat along the c axis in $\text{Bi}_2\text{Sr}_2\text{CaCu}_2\text{O}_8$ couple only very weakly to the conduction electrons, or that the scattering of the phonons is overshadowed by scattering of the phonons by other excitations or defects. In the defect scattering dominated case, it becomes difficult to extract an effective electron-phonon coupling constant from κ_c . In a previous analysis of κ_{ab} in $\text{Bi}_2\text{Sr}_2\text{CaCu}_2\text{O}_8$, it was found that near T_c phonons carrying heat in the ab plane are twice as likely to be scattered by (ab -plane) defects than by electrons.⁶

We now turn to a more detailed examination of the thermal conductivity of $\text{Bi}_2\text{Sr}_2\text{CaCu}_2\text{O}_8$. In our previous work⁶ on the ab -plane thermal conductivity of $\text{Bi}_2\text{Sr}_2\text{CaCu}_2\text{O}_8$, an analysis was used which took both electron and phonon contributions to κ_{ab} into account. The data were found to be consistent with a BCS-like description of κ in the superconducting state. In the present case, a similar analysis is not fruitful since κ_c is unaffected by the superconducting transition.

Recently, Tewordt and Wölkhausen⁷ (TW) have extended the theory of thermal conductivity in a BCS superconductor to the high- T_c oxides. Only the phonon contribution to the thermal conductivity is considered. In their isotropic model, the phonon thermal conductivity may be expressed as⁷

$$\kappa_{(\text{phonon})} = (4\pi/3)^{1/3} (2\pi)^{-1} (2\pi k_B^2 \Theta v_p / ha^2) (T/\Theta)^3 \times \int_0^{\Theta/T} \tau(z) [z^4 e^z / (e^z - 1)^2] dz, \quad (2)$$

where Θ is the Debye temperature, a is an average lattice constant, v_p is the phonon velocity, $\tau^{-1}(z)$ is the sum of frequency-dependent phonon scattering rates from different scattering processes, and $z = h\omega/2\pi k_B T$ with ω the phonon frequency. Equation (2) has been applied⁵ to both the in-plane and out-of-plane thermal conductivity of $\text{La}_{1.96}\text{Sr}_{0.04}\text{CuO}_4$, where phonon contributions to κ are suggested to dominate in both crystallographic directions. The out-of-plane phonon scattering is found to be dominated by stacking faults for this material.

TW have also examined theoretically⁸ the anisotropic phonon thermal conductivity for materials exhibiting both weak and strongly coupled superconductivity. (In the absence of any electron-phonon coupling, the anisotropic theory reduces to the isotropic case.) For a given set of model parameters, TW find that both κ_c and κ_{ab} show bumplike anomalies just below T_c . The anomaly in κ_c is markedly smaller. It is also predicted that κ_c exceeds κ_{ab} both in the normal and superconducting states, for weak as well as for strongly coupled superconductors.

Our κ_c data for $\text{Bi}_2\text{Sr}_2\text{CaCu}_2\text{O}_8$ presented in Fig. 1(a) is phonon dominated, and thus these data can be compared directly to the predictions of the TW theory. The lack of a substantial anomaly at T_c appears inconsistent with the model regardless of coupling strength. However, this discrepancy may be due to an unexpectedly large anisotropy in the phonon relaxation rate, as has been suggested⁸ by TW to account for the lack of a κ_c anomaly in $\text{YBa}_2\text{Cu}_3\text{O}_7$. Perhaps a more serious problem lies in the magnitude of the predicted κ_{ab}/κ_c anisotropy. In $\text{Bi}_2\text{Sr}_2\text{CaCu}_2\text{O}_8$ a room-temperature anisotropy of the measured thermal conductivity $\kappa_{ab}/\kappa_c \approx 6$ is found. Subtracting off electronic contributions, this ratio reduces to $\kappa_{ab(\text{phonon})}/\kappa_{c(\text{phonon})} \approx 4$, approximately independent of temperature from room temperature to T_c . It is difficult to reconcile the dominance of $\kappa_{ab(\text{phonon})}$ over $\kappa_{c(\text{phonon})}$ with the predictions of TW, unless different weights for different scattering mechanisms are assumed for in-plane and out-of-plane directions (a not unreasonable assumption).

It is straightforward to apply Eq. (2) to our measured κ_c in $\text{Bi}_2\text{Sr}_2\text{CaCu}_2\text{O}_8$. Assuming that the phonon scattering is dominated by stacking faults, $\tau^{-1}(z)$ in Eq. (2) reduces to

$$\tau^{-1}(z) = (0.7)(6\pi^2)^{2/3} \gamma^2 N_s v_p (T/\Theta)^2 z^2, \quad (3)$$

where γ is the Grüneisen constant and N_s is the number of stacking faults crossing a line of unit length. With $\Theta = 230$ K appropriate to $\text{Bi}_2\text{Sr}_2\text{CaCu}_2\text{O}_8$,¹⁶ the functional form of Eq. (2) is fixed, aside from an overall magnitude scaling factor. The solid line in Fig. 1(a) shows Eq. (2) fit to the κ_c data. We remark that the functional form of the calculated κ_c is rather sensitive to Θ , and the best

fit is obtained with the independently evaluated Θ for this material (a 50-K change in Θ visibly degrades the fit). The overall scaling factor allows the c -axis concentration to be evaluated explicitly; with $\gamma \approx 1$ and $a = 30.7 \times 10^{-8}$ cm, the curve in Fig. 1(a) gives a concentration of 1.3×10^4 stacking faults per cm.

We now turn to a brief discussion of the unusual c -axis electrical resistivity of $\text{Bi}_2\text{Sr}_2\text{CaCu}_2\text{O}_8$, as shown in Fig. 2. Various models have been proposed for the nonmetallic out-of-plane conduction of the high- T_c oxides, including interplanar holon tunneling¹⁷ and percolation conduction enhanced by defect scattering.¹⁸ A simple empirical expression found to account well for c -axis electrical conductivity in $\text{YBa}_2\text{Cu}_3\text{O}_{7-y}$ is¹⁴

$$\rho(T) = \rho_0 T^{0.7} \exp(\Delta/k_B T), \quad (4)$$

where Δ is a small characteristic “activation” energy analogous to that found in amorphous semiconductors. The solid line in Fig. 2 is Eq. (4) with $\rho_0 = 3.32 \times 10^{-2} \Omega \text{ cm K}^{-0.7}$ and $\Delta = 8.77$ meV. Between room temperature and ~ 100 K, Eq. (4) accounts extremely well for the c -axis electrical conduction in $\text{Bi}_2\text{Sr}_2\text{CaCu}_2\text{O}_8$. Between 100 K and T_c the model curve deviates from the experimental data; it is interesting to note that in precisely this temperature range the ab -plane electrical resistivity deviates from a purely linear temperature dependence. We thus find that the simple empirical expression Eq. (4), which accounts well for electrical transport in $\text{YBa}_2\text{Cu}_3\text{O}_{7-y}$, also applies to $\text{Bi}_2\text{Sr}_2\text{CaCu}_2\text{O}_8$ in the normal state over a wide temperature range.

Finally, we mention that the anisotropic transport of $\text{Bi}_2\text{Sr}_2\text{CaCu}_2\text{O}_8$ is extremely sensitive to the oxygen configuration of the specimen.^{6,19} With decreasing oxygen content, both the in-plane resistivity and in-plane thermoelectric power (TEP) tend toward the measured out-of-plane resistivity and out-of-plane TEP of fully oxygenated samples.¹⁹ For thermal transport, κ_{ab} for oxygen-deficient $\text{Bi}_2\text{Sr}_2\text{CaCu}_2\text{O}_8$ crystals is qualitatively very similar to κ_c reported here for fully oxygenated specimens.⁶ Both the in-plane electrical and in-plane thermal transport properties of oxygen-deficient $\text{Bi}_2\text{Sr}_2\text{CaCu}_2\text{O}_8$ crystals thus resemble the out-of-plane behavior of fully oxygenated crystals. A related question is how the out-of-plane thermal transport of $\text{Bi}_2\text{Sr}_2\text{CaCu}_2\text{O}_8$ changes with oxygen configuration. Such experiments are presently underway.

We thank M. L. Cohen for useful discussions, and L. Tewordt, N. P. Ong, and A. Kapitulnik for making manuscripts of their work available prior to publication. We are indebted to G. Briceno, K. Goldberg, A. Y. Liu, and X.-D. Xiang for technical assistance. This work was supported by the Director, Office of Energy Research, Office of Basic Energy Sciences, Materials Sciences Division of the U. S. Department of Energy under Contract No. DE-AC03-76SF00098. M. F. C. acknowledges support from the Department of Education.

- ¹S. W. Tozer, A. A. Kleinsasser, T. Penney, D. Kaiser, and F. Holtzberg, *Phys. Rev. Lett.* **59**, 1768 (1987).
- ²S. Martin, A. T. Fiory, R. M. Fleming, L. F. Schneemeyer, and J. V. Waszczak, *Phys. Rev. Lett.* **60**, 2194 (1988).
- ³P. B. Allen, W. E. Pickett, and H. Krakauer, *Phys. Rev. B* **37**, 7482 (1988).
- ⁴S. J. Hagen, Z. Z. Wang, and N. P. Ong, *Phys. Rev. B* **40**, 9389 (1989).
- ⁵D. T. Morelli, G. L. Doll, J. Heremans, M. S. Dresselhaus, A. Cassanho, D. R. Gabbe, and H. P. Jenssen, *Phys. Rev. B* **41**, 2520 (1990).
- ⁶M. F. Crommie and A. Zettl, *Phys. Rev. B* **41**, 10978 (1990).
- ⁷L. Tewordt and Th. Wölkhausen, *Solid State Commun.* **70**, 839 (1989).
- ⁸L. Tewordt and Th. Wölkhausen, *Solid State Commun.* **75**, 515 (1990).
- ⁹J.-M. Imer *et al.*, *Phys. Rev. Lett.* **62**, 336 (1989).
- ¹⁰M. F. Crommie, G. Briceno, X.-D. Xiang, and A. Zettl (unpublished).
- ¹¹S. D. Peacor and C. Uher, *Phys. Rev. B* **39**, 11559 (1989); D. T. Morelli, J. Heremans, and D. E. Swets, *ibid.* **36**, 3917 (1987); C. Uher and A. B. Kaiser, *ibid.* **36**, 5680 (1987); U. Gottwick *et al.*, *Europhys. Lett.* **4**, 1183 (1987).
- ¹²J. T. Fanton, A. Kapitulnik, D. B. Mitzi, B. T. Khuri-Yakub, and G. S. Kino (unpublished).
- ¹³H. C. Montgomery, *J. Appl. Phys.* **42**, 2971 (1971).
- ¹⁴M. F. Crommie, Amy Y. Liu, A. Zettl, Marvin L. Cohen, P. Parilla, M. F. Hundley, W. N. Creager, S. Hoen, and M. S. Sherwin, *Phys. Rev. B* **39**, 4231 (1989).
- ¹⁵J. R. Cooper, L. Forro, and B. Keszei, *Nature* **343**, 444 (1990).
- ¹⁶J. S. Urbach, D. B. Mitzi, A. Kapitulnik, J. Y. T. Wei, and D. E. Morris, *Phys. Rev. B* **39**, 12391 (1989).
- ¹⁷P. W. Anderson and Z. Zou, *Phys. Rev. Lett.* **60**, 132 (1988).
- ¹⁸J. C. Phillips, *Physics of High- T_c Superconductors* (Academic, Boston, 1989).
- ¹⁹M. F. Crommie, Amy Y. Liu, Marvin L. Cohen, and A. Zettl, *Phys. Rev. B* **41**, 2526 (1990).